INDC(YUG)-5/L

INDC(YUG)-5/L

International Atomic Energy Agency

INDC INTERNATIONAL NUCLEAR DATA COMMITTEE

MEASUREMENTS OF 14 MEV NEUTRON RADIATIVE CAPTURE γ-RAY SPECTRA AND INTEGRATED CROSS SECTIONS IN Sc, Y, Pr AND Ho

M. Budnar, F. Cvelbar, A. Likar, R. Martincic,
M. Potokar and V. Ivkovic

Report to the International Atomic Energy Agency

univerza v ljubljani

institut "jožef stefan" ljubljana, jugoslavija

January 1977

IAEA NUCLEAR DATA SECTION, KÄRNTNER RING 11, A-1010 VIENNA

Reproduced by the IAEA in Austria
January 1977

76-11232

INDC(YUG)-5/L

MEASUREMENTS OF 14 MEV NEUTRON RADIATIVE CAPTURE γ-RAY SPECTRA AND INTEGRATED CROSS SECTIONS IN Sc, Y, Pr AND Ho

M. Budnar, F. Cvelbar, A. Likar, R. Martincic,
M. Potokar and V. Ivkovic

Report to the International Atomic Energy Agency

January 1977

ACKNOWLEDGMENT

The measurements of 14 Mev neutron radiative capture γ- ray spectra and integrated cross section in Sc, Y, Pr and Ho presented here were performed with targets loaned to the J.Stefan Institute - Ljubljana by the International Atomic Energy Agency - Vienna, through the targets and samples exchange program.

The Agency not only ordered the materials, but also covered the expenses of their encapsulation. Its help is greatly appreciated.

We are also indebted to the Agency Officers Dr.L.Hjärne and Dr.C.R.O'Neal for their patience and vast correspondence.

The data is available as EXFOR 30364.

CONTENTS: Page

ABSTRACT

Gamma ray spectra and integrated cross sections for radiative capture in ^{45}Sc, ^{89}Y, ^{41}Pr and ^{165}Ho have been measured. Obtained integrated cross sections (800 $\pm$ 110)μb, (1490 $\pm$ 210)μb, (980 $\pm$ 160)μb and (940 $\pm$ 150)μb are in accordance with measurements at other elements showing smooth mass dependence.

Measuring procedure and experimental data evaluation is described in details.

1. INTRODUCTION

In the last decade much effort has been devoted to the study of radiative capture of energetic neutrons[1-10].

The reason for this is the improvement of experimental techniques, theoretical models and rising interest in 14 MeV neutron cross section data which are closely connected with fusion problems.

Among available 14 MeV neutron capture data there are a lot of γ-ray spectra, integrated and activation cross sections for various nuclei[11-45].

Data for Sc, Y, Pr and Ho obtained in this work can be incorporated into a series of systematic measurements relating to atomic number and serve also for testing theoretical models for capture of 14 MeV neutrons. At the same time, the cross sections and γ-ray spectra for Pr and Ho at least partly fill an overall deficiency of neutron data in the rare earth area.

2. EXPERIMENT

A schematic diagram of the experimental set-up is shown in Fig. 1. The neutron source is placed at the centre of the sample. In such geometry one obtains the maximum yield of γ-rays from the sample and the optimal ratio of the number of these γ-rays to the number of γ-rays from other sources. This arrangement, on the other hand, allows only poor shielding of the spectrometer against neutrons. Consequently, high background due to neutron interactions in scintillators is expected. However, by the use of the scintillation telescope pair spectrometer[46,47], the number of background pulses is reduced appreciably.

2.1. Neutron source

Neutrons are produced by the bombardment of tritium target by 100 keV deuterons from a Cockroft-Walton accelerator. The

neutron flux from the source is $\sim 10^8$ (1 ± 0.10) neutrons/sec. The angular distribution of neutrons is nearly isotropic. The average neutron energy is 14.1 MeV and the energy spread is 1.35 MeV.

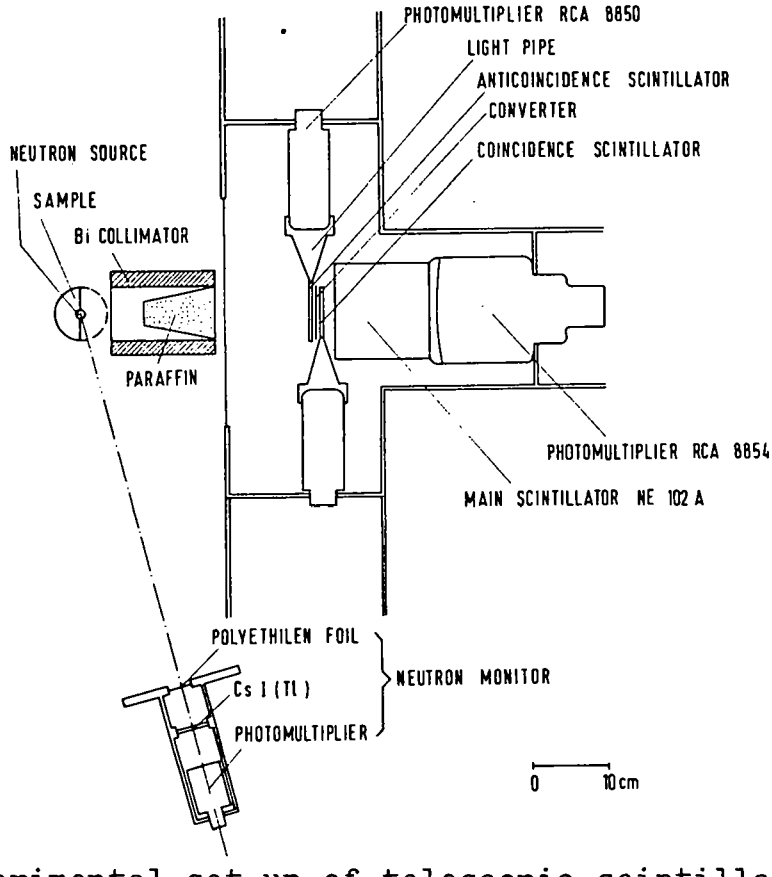

Fig. 1: Experimental set-up of telescopic scintillation pair spectrometer and neutron monitor in measurements of γ-ray spectra from the radiative capture of 14.1 MeV neutrons.

2.2. Samples

The samples are spheres or hemispheres with diameter 5-6 cm and with a hole 10 mm diameter to the centre of the sample fitting the tritium target holder. Hemispheres are used for high-Z targets instead of spheres in order to reduce the self-absorption of capture γ-rays and the absorption of γ-rays coming from the target holder. Samples are cast, turned from metallic block or prepared by compression of the powder or

shavings under high pressure into thin (0.2 mm) capsules. Sample materials of natural isotopic composition are used. From the geometry of the experiment, it follows that the measured spectra are integrated over a solid angle of 4π when spherical samples are used or 2π when hemispheres are measured. The angle between the direction of the neutrons and the corresponding capture γ-rays ranges from 0 to π in the first case, or $1/2\pi$ to π in the second case.

2.3. Spectrometer

Prompt γ-rays from the capture of 14.1 MeV neutrons in various samples are measured by a telescopic scintillation pair spectrometer (TSPS). Gamma rays create electron-positron pairs in a lead foil named the converter. The energy of the pairs is absorbed in a main scintillator (MS) made from NE 102A plastic. Two thin plastic scintillators named the coincidence (Co) and anticoincidence (A) scintillator, together with a fast (nanosecond) coincidence-anticoincidence electronic circuit, act as a shield for the spectrometer against undesired events (Compton electrons, mesons). A telescopic arrangement of the scintillators makes the spectrometer sensitive to γ-rays from the face side only.

The resolution of the spectrometer is 12.5 %, 9.5 % and 8.0 % for γ-ray energies of 12.1 MeV, 16.5 MeV and 20.4 MeV, respectively. The efficiency of the spectrometer at these energies is 0.45 %, 0.55 % and 0.56 %, respectively. A low tail in the response function of the spectrometer makes it possible to obtain the γ-ray spectrum from the measured distribution with a relatively small correction.

2.4. Electronics

The block diagram of the spectrometer and neutron monitor is shown in Fig. 2. Anode pulses from the main photomultiplier are lead through a linear gate and biased amplifier to an analog-to-digital converter. Anode pulses from all three photomultipliers are discriminated and shaped by fast discriminators and fed to a fast-coincidence unit. The output pulses

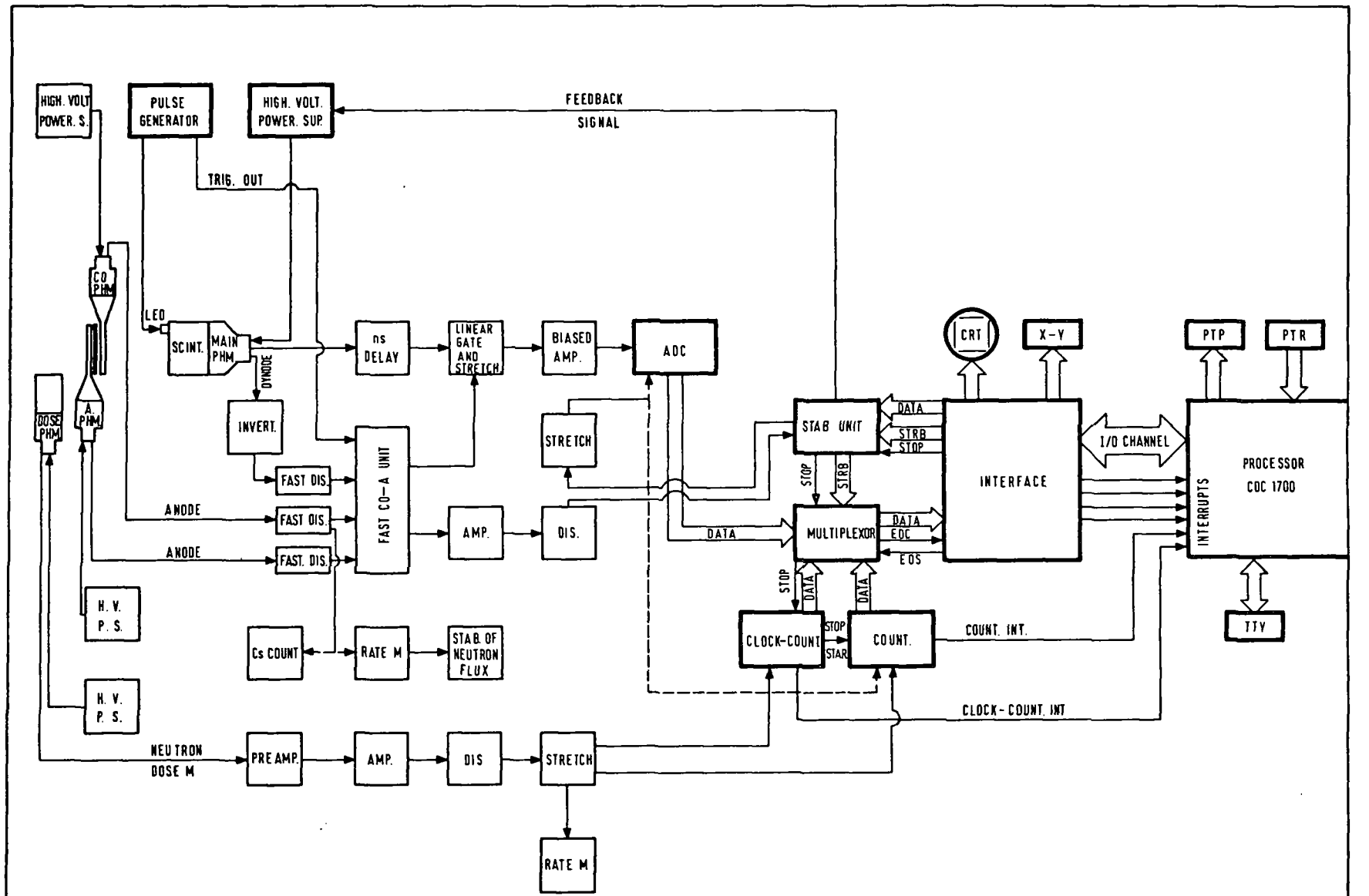

Fig. 2: Block scheme of electronics for telescopic scintillation pair spectrometer, for neutron monitor and interface connection with the CDC mini computer.

from this unit open the fast linear gate for very short (40 ns) time intervals, which reduces the background appreciably. The ADC is triggered by a slow output of the coincidence-anticoincidence unit and digital information is then stored in the memory of a mini computer (CDC 1700). Measuring prompt γ -ray spectra from the radiative capture of 14 MeV neutrons with TSPS, the problem of photomultiplier instability caused by a high ($\sim$ 25 μA) anode current arises. Therefore a totally computer controlled gain stabilizing system was built[48,49]. The system uses a fast (ns) pulsed light emitting diode (MV 10B) as a stable reference to correct the gain of the photomultiplier and a mini computer for data acquisition and for photomultiplier high voltage control in a feedback loop. Stability of peak channel number to 0,3 % or better is obtained over extended periods of time without significant loos in resolution.

2.5. Energy calibration

The energy scale of the spectrometer is periodically calibrated with 11.7 MeV and 16.1 MeV gamma rays from the reaction $^{11}B(p,\gamma)^{12}C$ at a proton energy E_p = 163 keV. During the calibration, the spectrometer is irradiated with a radium source (20 μc) to keep the anode current from the photomultiplier the same as during the measurements with neutrons. At 10^8 neutrons/sec from the neutron source, there are about 10^5 recoil protons/sec in the main scintillator, which corresponds to about 30 μA anode current of the main photomultiplier. In this way we avoid changes in the amplification factor of the photomultiplier due to changes in the anode current. The accuracy of the calibrated energy scale resulting from this procedure is 1 % at 11.7 MeV and 3 % at 16.1 MeV.

2.6. Collimator

Between the neutron source and the spectrometer a bismuth collimator with inserted paraffin cone is placed (Fig. 1). This collimator appreciably attenuates gamma rays coming into the spectrometer from side directions. The paraffin cone attenuates

the neutron flux by a factor of 2 and lowers the background of the spectrometer by nearly this factor. The intensity of gamma rays directed towards the spectrometer is, on the other hand, attenuated only by 16 %. In the measurements of the elements Sc and Ho, we replaced the paraffin cone with a paraffin cylinder which fits the bismuth collimator hole and another one close to the anticoincidence scintillator. In this way, we increased the yield to background ratio by a factor of 2.

2.7. Neutron flux monitor

Neutron flux is monitored by a simplified recoil proton spectrometer, using a CsI(Tl) crystal as a proton detector (Fig. 1). By putting the monitor discriminating level below the main peak, practically all the recoils belonging to 14.1 MeV neutrons are recorded. The accuracy of the determination of the neutron flux is $\pm$ 6 %.

3. EXPERIMENTAL PROCEDURE

Measurements of the neutron capture γ-ray spectra were performed by alternating the"sample-in" and "sample-out" runs. The "sample-in" runs give a pulse height distribution M(k) which contains pulses from the capture gamma ray events in the sample as well as the background pulses. The "sample-out" runs give the background O(k), which corresponds to capture gamma ray events in the spectrometer and its surroundings, pile-up processes and chance coincidences in the spectrometer. For encapsulated targets, the "sample-out" run is the run with sample replaced by its capsule. The difference between the pulse height distributtions measured with the sample in the "in" and "out" positions is the distribution corresponding to the radiative capture of fast neutrons in the sample nuclei (this we call the measured distribution S(k)):

$$S(k) = M(k) - O(k) \qquad (1)$$

The effect to background ratio averaged over the whole spectrum is roughly 1 : 1.

4. BACKGROUND

The background part of the pulse height distribution in the "sample-in" runs is not the same as the background measured in the "sample-out" runs. The difference results from the absorption of part of background gamma rays in the sample and from the fact that the neutron flux is reduced due to the presence of the sample.

For proper background correction one needs to know (see Fig. 3) the part originating in the walls of the experimental room $A_w(k)$, the part coming from the target holder $A_t(k)$ and the rest $B(k)$. The last part contains all gamma rays which do

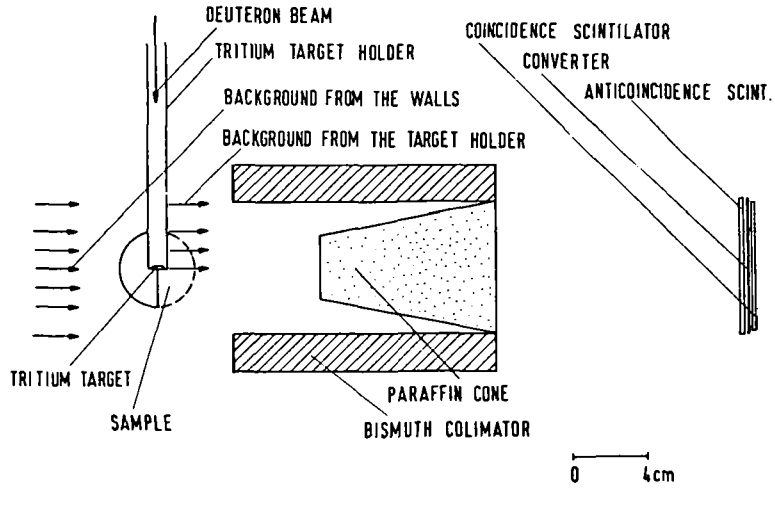

Fig. 3: Division of the background.

not fall on the converter through the hole of the bismuth collimator and other events (pile-up in the spectrometer, chance coincidences, natural background). The background is therefore the sum:

$$O(k) = A_w(k) + A_t(k) + B(k) \qquad (2)$$

Particular constituents were estimated numerically.

4.1. Background from the target holder $A_t(k)$

The target holder is a 0.5 m long, 10 mm diameter iron tube holding a copper cup with a copper tritium target backing soldered in it (Fig. 4). Tritium is adsorbed in a thin tantalum (Ta) layer vacuum deposited on the copper backing 0.4 mm thick.

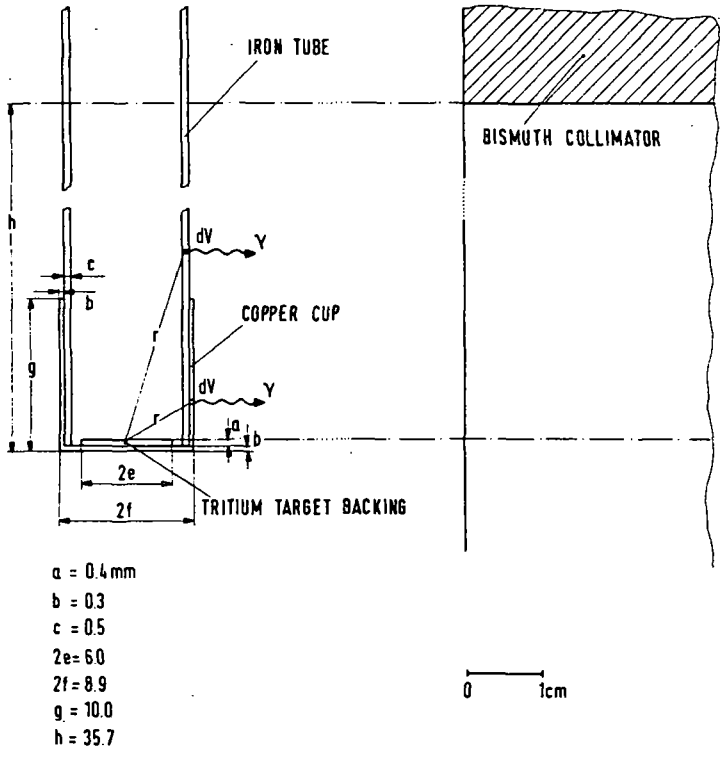

Fig. 4: Geometry of the tritium target holder.

The number of gamma rays with energies between E_γ and $E_\gamma + dE_\gamma$ from the holder volume element dV which enter the sensitive area of the spectrometer, if I_o neutrons are produced in the neutron source, is:

$$d\left(\frac{dN}{dE_\gamma}\right) = \frac{I_o}{4\pi r^2} \cdot ndV \cdot \frac{d\sigma}{dE_\gamma} \cdot \frac{\Omega^*}{4\pi} \cdot \eta_{par} \cdot \eta_{TSPS} \quad , \qquad (3)$$

I_o = number of 14 MeV neutrons from the neutron source in solid angle 4π .

r = distance between the neutron source and volume element dV

n = density of nuclei $[cm^{-3}]$

dV = target holder volume element

$\frac{d\sigma}{dE_\gamma}$ = differential neutron capture cross sections in iron or copper

$\frac{\Omega^*}{4\pi}$ = relative spectrometer solid angle

$\frac{\Omega^*}{4\pi} = 3.09 \cdot 10^{-3} \ (1 \pm 0.02)$

η_{par} = absorption factor for gamma rays in the paraffin cone

$\eta_{par} = 0.92 \ (1 \pm 0.01)$

η_{TSPS} = efficiency of the spectrometer

$\eta_{TSPS} = 0.55 \cdot 10^{-2} \ (1 \pm 0.03)$

The yield of gamma rays from the target holder was calculated taking into account the following assumptions:

- the self absorption of gamma rays in the target holder can be neglected
- the attenuation of neutrons in the target holder is insignificant
- the spectrometer solid angle was taken to be the same for all target holder elements
- the neutron source is a point source
- expression (3) was integrated only over that part of the target holder which is seen from the converter through the bismuth collimator hole.

The number of gamma rays in the energy interval E_γ, $E_\gamma + dE_\gamma$ from the target holder is then:

$$\frac{dN}{dE_\gamma} = \frac{I_0}{4\pi} n \frac{d\sigma}{dE_\gamma} \cdot \frac{\Omega^*}{4\pi} \cdot \eta_{par} \cdot \eta_{TSPS} \cdot \iint d\Omega \, .dr \qquad (4)$$

$$J = \frac{1}{4\pi} \iint d\Omega \, .dr \qquad (5)$$

Integrals for the particular parts of the target holder were calculated numerically. The results are:

Iron tube	J = 0.039 cm
Copper cup	J = 0.051 cm
Backing	J = 0.060 cm

Differential capture cross sections for iron and copper were measured in our laboratory several years ago. As background corrections are small for low Z nuclei, we did not recalculate

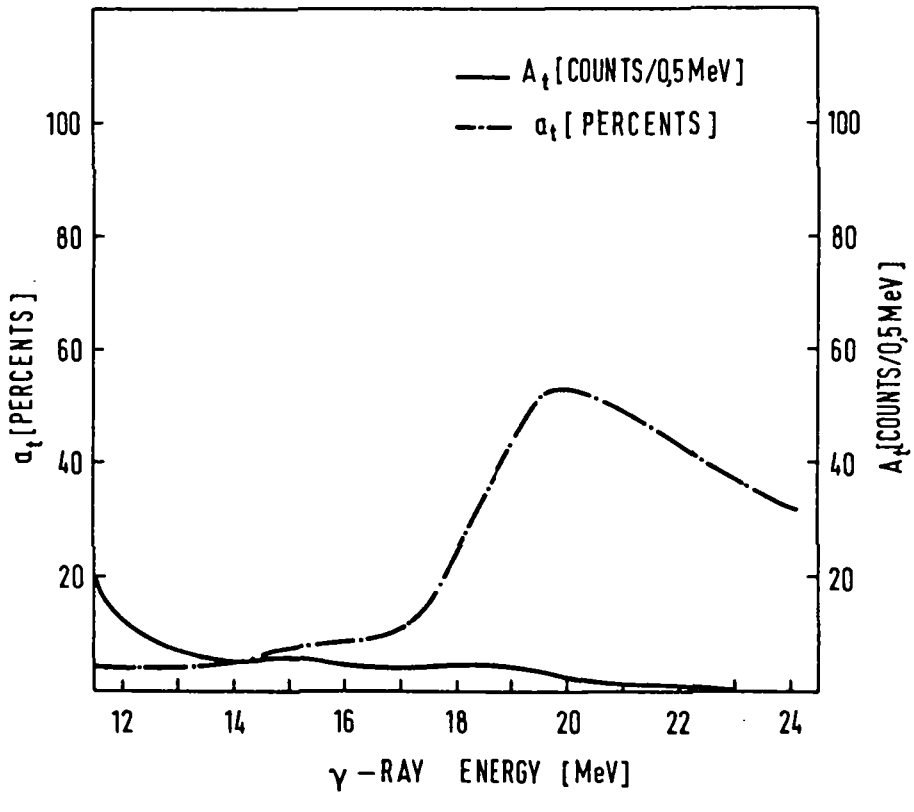

Fig. 5: Relative ($a_t(k)$) and absolute ($A_t(k)$) background from the tritium target holder averaged over a series of measurements.

cross sections for Fe and Cu with background parts gained in this work. The error in cross sections for iron and copper made with this procedure is within experimental error. The absolute and relative yields of gamma rays from the target holder are shown in Fig. 5 and Table 1.

E(MeV)	Channels	a_t(%)	b(%)
10,75	17 - 18	5	95
11,25	19 - 20	5	95
11,75	21 - 22	4	96
12,25	23 - 24	4	96
12,75	25 - 26	4	96
13,25	27 - 28	4	96
13,75	29 - 30	4	96
14,25	31 - 32	5	95
14,75	33 - 34	7	93
15,25	35 - 36	8	92
15,75	37 - 38	8	92
16,25	39 - 40	9	91
16,75	41 - 42	9	91
17,25	43 - 44	12	88
17,75	45 - 46	19	81
18,25	47 - 48	29	71
18,75	49 - 50	38	62
19,25	51 - 52	48	52
19,75	53 - 54	53	47
20,25	55 - 56	52	48
20,75	57 - 58	50	50
21,25	59 - 60	48	52
21,75	61 - 62	45	55
22,25	63 - 64	41	59
22,75	65 - 66	38	62
23,25	67 - 68	36	64
23,75	69 - 70	33	67
24,25	71 - 72	32	68

Table 1: Part of the background due to the sample holder $a_t(k)$ and rest of the background b(k), both relative to the total background.

The background from the target holder represents on average about 15 % of the total background and is determined with an accuracy of ± 25 %. This overall error results from the uncertainity:

- in the capture cross sections for iron and copper ± 20 %
- in the calculation of integrals 10 %
- in the solid angle $\frac{\Omega^*}{4\pi}$ 2 %
- in the neutron flux determination ± 6 %
- of the efficiency of the spectrometer ± 3 %
- of the absorption of gamma rays in the paraffin cone ± 1 %

4.2. Background from the walls of experimental room $A_w(k)$

The number of gamma rays from the borated paraffin wall volume element dV, if the number of neutrons from the neutron

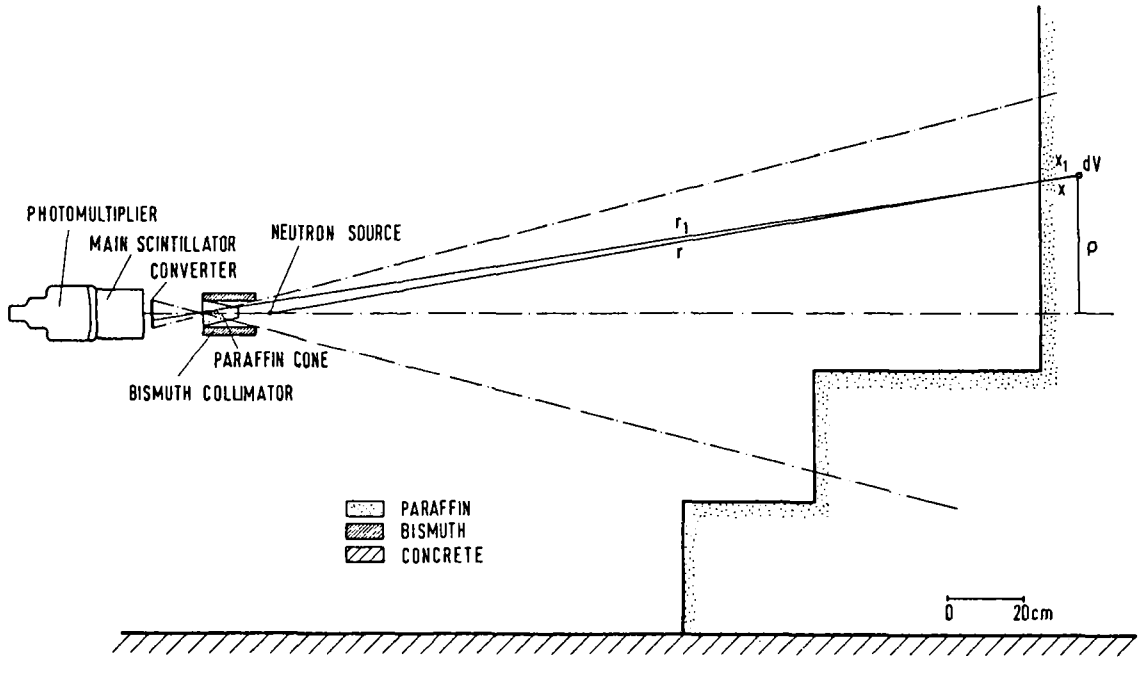

Fig. 6: Geometry of the walls of experimental room

source is I_o, can be written (Fig. 6):

$$dN = \frac{I_o}{4\pi r^2} \cdot e^{-n\sigma_{non} x_1} \cdot (n_C \cdot \sigma_C + n_H \cdot \sigma_H) \cdot dV \cdot e^{-\mu x_2} \cdot \left(\frac{S_{eff}}{4\pi r^2}\right) \cdot \eta_{par} \cdot \eta_{TSPS} \qquad (6)$$

I = number of neutrons from the neutron source in 4
r = distance between the neutron source and the volume element dV
$n\sigma_{non}$ = macroscopic nonelastic cross section for 14 MeV neutrons in paraffin
x_1 = path of neutrons in the paraffin wall
n_c, n_H = density of hydrogen and carbon nuclei $[cm^{-3}]$
x_2 = path of gamma rays in the paraffin wall
μ = absorption coefficient for gamma rays in the paraffin
S_{eff} = effective spectrometer area seen from the volume element dV
r_1 = distance between volume element dV and the converter
η_{par} = absorption factor for gamma rays in the paraffin cone
η_{TSPS} = efficiency of the spectrometer
σ_c, σ_H = integrated cross sections for the capture of 14 MeV neutrons in carbon and hydrogen

$\sigma_c = 200\,\mu b$, $\sigma_H = 80\,\mu b$

Integration over the volume which contributes to the background $A_w(k)$ was made graphically. As the calculation shows that the contribution of gamma rays from the walls of the experimental room is less then 1 % of the total background, it was not taken into account. Also the corresponding contribution due to slowed down neutrons in the paraffin walls was not considered either.

The rest of the background named B(k) is then the difference between the total background O(k) and the background from the target holder:

$$B(k) = O(k) - A_t(k) \qquad (7)$$

Its absolute and relative values are shown in Fig. 7 and Table 1.

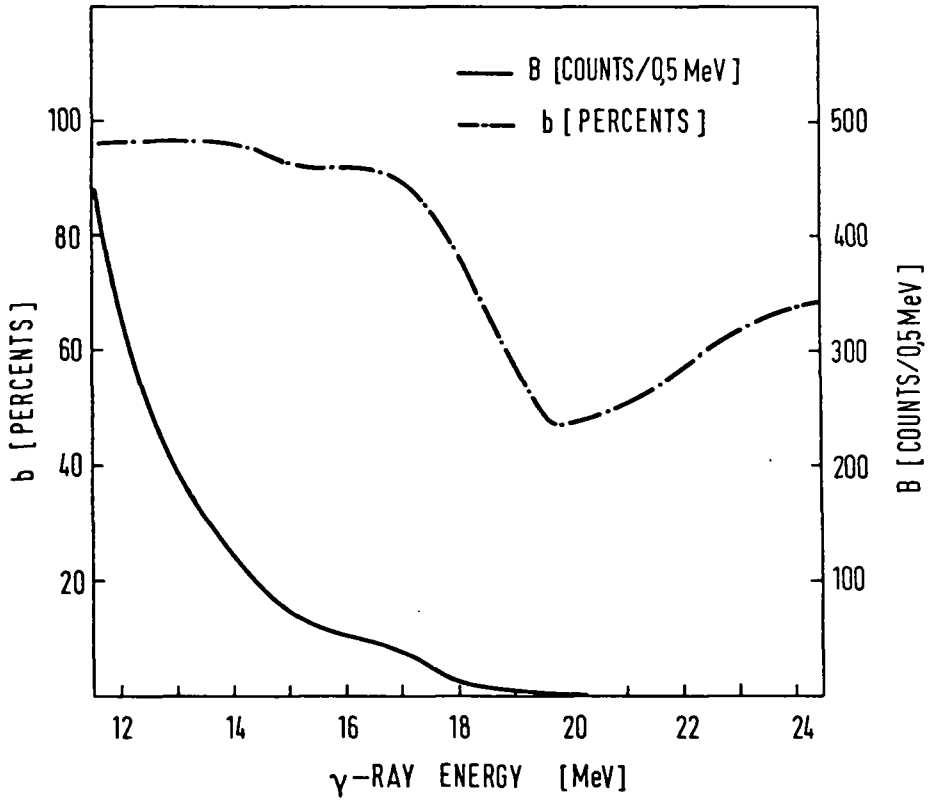

Fig. 7: Relative (b(k)) and absolute (B(k)) rest of the background averaged over a series of measurements.

5. CORRECTION OF THE MEASURED PULSE HEIGHT DISTRIBUTION

A number of corrections are necessary before the cross section for the capture of fast neutrons can be obtained from the measured spectra. First we have to account for the background correction.

To obtain the spectrum of γ-rays, the measured pulse height distribution is unfolded for the response function of the spectrometer, which also includes the efficiency of the spectrometer.

To obtain the cross section it is in adition necessary to consider self absorption of gamma rays, absorption of gamma rays in paraffin cone and correction of neutron flux due to nonelastic processes in the sample.

A path from measured pulse height distributions and measured number of neutrons to the differential and integrated cross section is schematically shown in the flow chart (next page).

5.1. Background corrections

5.1.1. Corrections for a spherical sample

The sphere of sample material is placed around the tritium target holder as shown in Fig. 3. In this geometry the flux of 14 MeV neutrons from the neutron source is attenuated due to inelastic scattering, (n,2n) reactions and other reactions before it reaches the neutron monitor. Neutrons from these processes have energies of about 1 MeV and are not detected by the neutron monitor. If an equal number of 14 MeV neutrons is detected with by the neutron monitor in "sample in" run as in "sample out" run, the number of neutrons in the neutron source is increased in the "in" run by a factor $e^{n\delta_{non}R}$, where $n\delta_{non}$ is the macroscopic nonelastic cross section for the 14 MeV neutrons in the sample and R is the sample radius. The experimental room, on the other hand, is exposed to the same number of neutrons in the "sample in" and in the "sample out" runs.

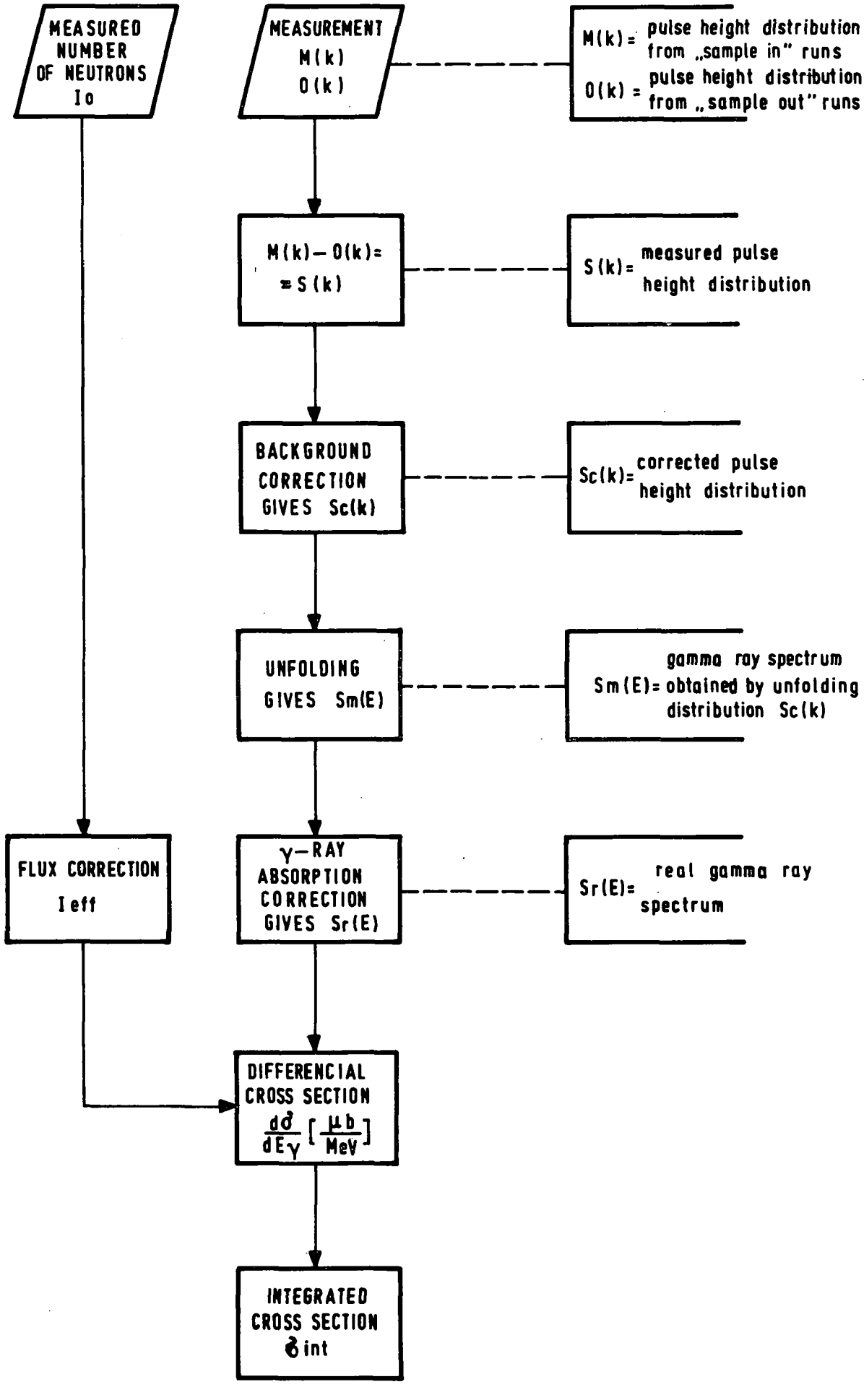
MEASURED NUMBER OF NEUTRONS Io
MEASUREMENT M(k) O(k)
M(k) = pulse height distribution from „sample in" runs
O(k) = pulse height distribution from „sample out" runs
M(k) − O(k) = = S(k)
S(k) = measured pulse height distribution
BACKGROUND CORRECTION GIVES Sc(k)
Sc(k) = corrected pulse height distribution
UNFOLDING GIVES Sm(E)
Sm(E) = gamma ray spectrum obtained by unfolding distribution Sc(k)
FLUX CORRECTION Ieff
γ−RAY ABSORPTION CORRECTION GIVES Sr(E)
Sr(E) = real gamma ray spectrum
DIFFERENCIAL CROSS SECTION dσ/dEγ [μb/MeV]
INTEGRATED CROSS SECTION σint

Let us consider the change of particular background components between measurements with a spherical sample:

- The background from the target holder is enlarged because of the enlarged number of neutrons from the neutron source, as follows from the above discussion. We have also to consider the absorption of target holder gamma rays in the sample. In the aproximation that gamma rays are directed parallel to the axis of the spectrometer, this absorption is described by a factor $e^{-\mu(R-R_1)}$, where μ is the absorption coefficient for gamma rays in the sample, R_1 is the radius of the hole in the sample and R is the sample radius.
- The background component from the walls is lower than 1 % of the background and can be neglected.
- The number of 14 MeV neutrons on parts of experimental area which are the source of the part B(k) is the same as in the "sample-out" runs. If part B(k) originates from events caused by 14 MeV neutrons, we cannot expect a change in this part of the background. The error made by this assumption is less then 5 %.

The measured pulse height distribution has to be corrected only for the change in the target holder part of the background. It follows:

$$S_c(k) = M(k) - \eta(k) \cdot O(k) \tag{8}$$

$S_c(k)$ = corrected measured pulse height distribution S(k)

$\eta(k)$ = background correction factor

$$\eta(k) = a_t(k) . e^{-\mu(R-R_1)} . e^{n\delta_{non}R} + b(k) \tag{9}$$

$$a_t(k) = \frac{A_t(k)}{O(k)}$$

$$b(k) = \frac{B(k)}{O(k)} \tag{10}$$

The corrected measured pulse height distribution $S_c(k)$ represents a distribution of gamma rays originating in the sample and interacting with the spectrometer during the time of the measurement.

The error of distribution $S_c(k)$ includes the statistical error of the distribution M(k), the statistical error of the distribution $\eta(k).O(k)$ and uncertainity in the background correction factor $\eta(k)$.

$$\delta^2 = M(k) + \eta^2(k)\, O(k) + [\Delta\eta(k).O(k)]^2 \qquad (11)$$

The error of factor $\eta(k)$ was estimated to be $\pm$ 7 % and originates in the uncertainity of $A_t(k)$ (25 %), the uncertainity of the factor $e^{-\mu(R-R_1)}.e^{n\delta_{non}R}$ ($\pm$ 5 %) and the uncertainity in the change of B(k) between the "sample-in" runs ($\pm$ 5 %).

5.1.2. Corrections for a hemispherical sample

Measurements with hemispherical samples were performed with the same experimental set-up as for spherical ones (Fig. 3). The hemispherical sample is positioned so that its plane side faces the spectrometer. In this way the absorption of the background originating in the sample holder is avoided. Also the number of neutrons from the neutron source is the same as in the "sample out" runs. Background corrections are therefore unecessary in the case of hemispherical samples. The above assumptions are accurate in the range of 1 % of total background.

The overall error of the distribution $S_c(k)$ can be written:

$$\delta^2 = M(k) + O(k) + [1\ \% \ .\ O(k)]^2 \qquad (12)$$

As we have seen, the absence of a background correction strongly supports the choice of a hemispherical sample. Another argument is self-absorption in the sample which is strongly increased for high Z targets.

On the other hand, a choice of hemispheres means that we have to renounce the integration of an unknown γ-ray angular distribution over a solid angle of 4π. The measured cross sections are therefore experimentally integrated over 2π

$$\frac{d\sigma}{dE_\gamma} = 2 \cdot \int_{\vartheta=\pi/2}^{\vartheta=\pi} \frac{d^2\sigma}{dE_\gamma \cdot d\Omega} \cdot d\Omega \qquad (12)$$

This can introduce some error in a comparison between integrated cross sections measured with spheres or hemispheres, if the angular distribution is anisotropic.

5.2. Unfolding of the measured pulse height distribution

To obtain the spectrum of gamma rays interacting with the converter, the measured pulse height distribution has to be unfolded using the known response function of the spectrometer. The response function of the TSPS to monochromatic gamma rays has a relatively sharp peak [FWHM = (1.65 ± 0.05)MeV] and a rather low tail on the low energy side.

The gamma ray spectrum falling on the spectrometer can be obtained from the measured distribution by solving an integral equation. This can be done relatively simply by introduction of the response matrix M. A continuous gamma ray spectrum interacting with a converter can be treated as a vector $S_m(E)$ given in energy intervals ΔE. The measured pulse height distribution (corrected for the background correction) which belongs to the gamma ray spectrum is also considered as a vector $S_c(\varepsilon)$, where ε is the height of electrical pulses in MeV. Both vectors are connected with the response matrix of the spectrometer:

$$S_c(\varepsilon) = M \cdot S_m(E) \qquad (13)$$

Matrix elements are given by:

$$M_{ji} = \frac{\int_{\Delta\varepsilon_j} \int_{\Delta E_i} K(E,\varepsilon) \cdot d\varepsilon \, dE}{\Delta\varepsilon_j} \qquad (14)$$

where $K(E,\varepsilon)$ is the response function of the spectrometer. The response function of the spectrometer is determined with monochromatic gamma rays which have energies 12.1 MeV, 16.5 MeV and 20.3 MeV (Fig. 8). Values for other energies are obtained by interpolation or extrapolation with the parabolic aproximation. The response matrix also includes the efficiency of the spectrometer, but not the solid angle of the TSPS. Its values are given in Table 2 .

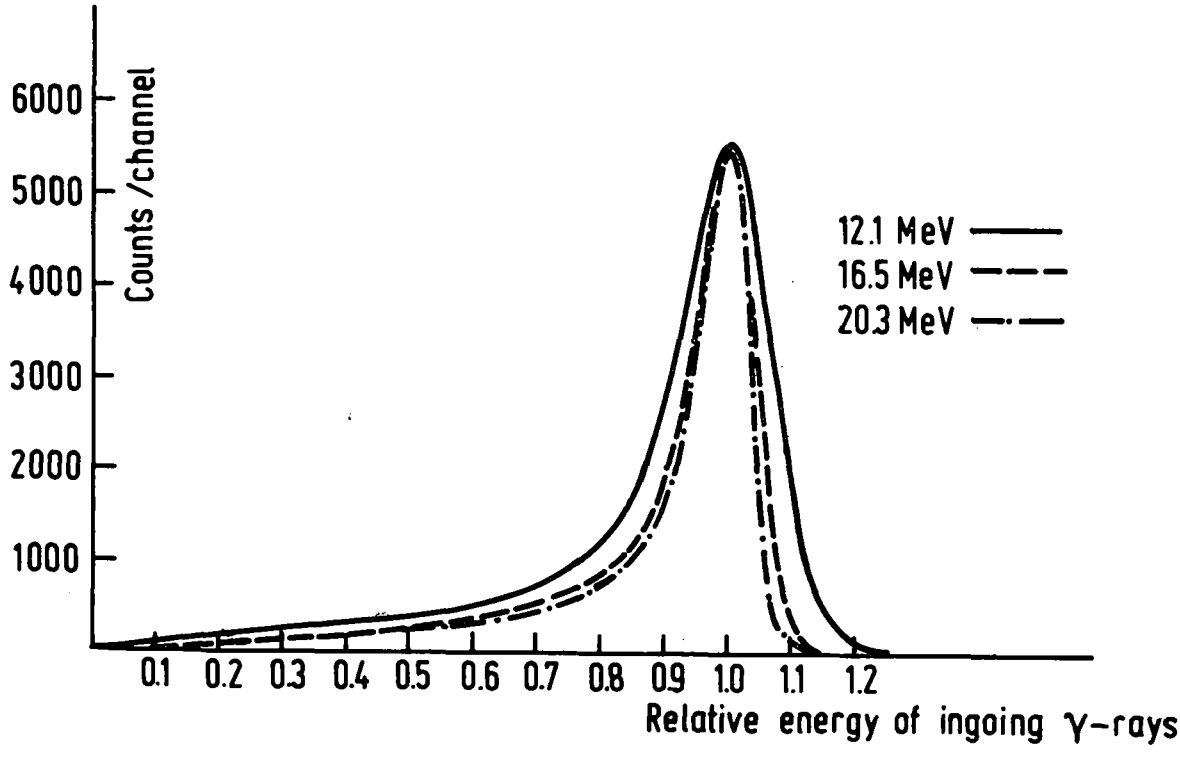

Fig. 8: Response function of the spectrometer TSPS.

From the corrected measured distribution $S_{\varepsilon}(\varepsilon)$ one can obtain the gamma ray spectrum $S_m(E)$ knowing the inverse matrix M^{-1}. Diagonal elements of the matrix M have maximal values, all other elements are small except those which are close to diagonal elements. Inverse matrix nondiagonal elements should all be negative and diagonal elements positive. Due to the uncertainity of the matrix elements, the inverse matrix elements alternate in sign. This has an undesired consequence that the

TABLE 2

Response function matrix.

ϵ \ k	11.25	11.75	12.25	12.75	13.25	13.75	14.25	14.75	15.25	15.75	16.25	16.75	17.25	17.75	18.25	18.75	19.25	19.75	20.25	20.75	21.25	21.75	22.25	22.75	23.25	23.75
11.25	874	743	493	312	221	172	141	119	102	88	77	69	62	56	52	50	47	46	44	42	41	39	37	36	35	34
11.75	639	883	758	508	323	229	178	146	124	106	91	80	71	63	58	53	50	48	47	45	43	41	40	38	37	35
12.25	254	639	890	779	522	333	236	183	151	128	110	95	83	73	65	60	55	52	50	47	45	43	42	40	39	37
12.75	55	263	638	903	800	538	343	243	189	155	132	113	98	85	76	67	62	57	53	50	48	46	44	42	41	39
13.25	9	63	270	638	915	821	553	353	249	193	160	136	116	101	89	78	70	63	59	55	51	48	46	45	43	41
13.75	2	11	68	270	637	929	842	569	362	256	199	164	140	120	104	92	81	72	66	60	56	52	49	47	45	43
14.25		2	14	72	263	633	944	863	585	372	261	203	168	143	124	108	94	83	74	67	61	57	53	50	47	45
14.75			3	16	74	261	631	958	884	598	384	269	208	171	147	127	110	97	86	76	69	63	58	54	51	48
15.25			1	4	18	73	255	631	971	904	613	392	276	213	175	149	130	114	100	89	78	71	65	60	55	52
15.75				1	5	19	71	249	632	983	922	632	399	279	217	178	152	133	116	102	91	81	72	66	61	56
16.25					1	5	19	66	243	634	996	938	649	412	286	222	183	155	135	119	104	93	83	74	68	63
16.75						2	5	18	60	235	637	1009	949	659	423	294	227	187	158	139	121	107	95	85	77	69
17.25							2	5	17	53	232	640	1017	955	667	430	300	231	191	161	140	124	109	97	87	79
17.75								2	5	14	46	229	642	1024	964	672	437	306	236	194	164	142	126	111	99	89
18.25								1	2	4	10	38	228	642	1030	966	678	441	312	240	198	167	144	127	114	102
18.75									1	1	2	7	33	226	645	1030	968	679	445	319	244	201	170	146	130	116
19.25												1	3	31	226	647	1032	964	680	450	324	248	203	173	149	131
19.75														2	30	227	652	1027	959	681	456	330	251	206	175	151
20.25															1	30	229	655	1022	954	684	462	335	255	209	178
20.75																1	33	231	658	1016	951	686	468	338	261	212
21.25																	3	37	232	658	1010	947	690	475	340	266
21.75																		6	45	236	658	1005	942	693	481	345
22.25																			11	48	242	658	995	933	698	485
22.75																			2	16	49	249	658	980	927	701
23.25																				4	18	49	260	657	969	920
23.75																				1	5	20	52	274	659	957

The tabulated values have to be multiplied by a factor 10^{-6}. k represents the center of the gamma ray energy interval (in MeV) and ϵ the center of the pulse height interval (in MeV).

error of $S_m(E)$ becomes quite large:

$$\{S_m(E)\}_j = \sqrt{\sum_i M^{-1}_{ij} \cdot (\{\Delta S_c(\varepsilon)\}_i)^2} \qquad (14)$$

To solve this problem we follow the Mollenauer iteration procedure[50,51]. Vector $S_c(\varepsilon)$ is multiplied by M to get a new distribution $S_c^{(1)}(\varepsilon) = M.S_c(\varepsilon)$. The ratio between $S_c^{(1)}(\varepsilon)$ and $S_c(\varepsilon)$ is approximately the same as the ratio between $S_c(\varepsilon)$ and $S_m(\varepsilon)$. Multiplying the i-th component of vector $S_c(\varepsilon)$ by the ratio $S_c(\ )_i$ / $M.S_c(\ )_i$ we get the i-th component of the first approximation to the vector $S_m(E)$ which we are looking for:

$$\{S_m^{(1)}(E)\}_i = \frac{(\{S_c(\varepsilon)\}_i)^2}{\{M.S_c(\varepsilon)\}_i} \qquad (15)$$

The first approximation $S_m^{(1)}(E)$ multiplied by matrix M is then approximated with $S_c(\varepsilon)$. If the difference is greater then the statistical error, the procedure is continued:

$$\{S_m^{(2)}(E)\}_i = \frac{\{S_c(\varepsilon)\}_i \cdot \{S_m^{(1)}(E)\}_i}{\{M.S_m^{(1)}(E)\}_i} \qquad (16)$$

Our procedure was terminated after the first step because the distribution $S_m^{(1)}(E)$ multiplied by matrix M was equal to the measured distribution $S_c(\varepsilon)$ within the statistical error of $S_c(\varepsilon)$.

In this procedure the statistical error grows from step to step. Calculation made with several different shapes for the measured distribution $S_c(\varepsilon)$ yielded an increase in statistical error by a factor of 1.8 in first step, almost undependent of the shape of the distribution $S_c(\varepsilon)$. The statistical error of the first approximation $S_m^{(1)}(E)$ is therefore increased by a factor of 1.8 relative to the statistical error of the measured distribution $S_c(\varepsilon)$.

5.3. Correction for the absorption of γ-rays

Gamma rays created in the sample are partially absorbed in the sample itself and in the paraffin cone.

The correction factor for self absorption in the sample is defined by the ratio

$$\eta_{sample} = \frac{S_r(E_\gamma)}{S_r'(E_\gamma)} \tag{17}$$

$S_r(E_\gamma)$ = the yield of gamma rays with energy E_γ created in the sample and directed towards the converter

$S_r'(E_\gamma)$ = gamma rays which actually leave the sample and are directed towards the convertor

If we assume that gamma rays are directed parallel to the axis of the spectrometer, we have for a sphere:

$$\eta_{sample} = \frac{2R}{\int_0^{\pi}\int_0^{R} e^{-\mu\rho\left(\sqrt{R^2 - r^2\sin^2\vartheta} - r\cos\vartheta\right)} \sin\vartheta \, d\vartheta \, dr} \tag{18}$$

and for a hemisphere:

$$\eta_{sample} = \frac{R}{\int_0^{\pi/2}\int_0^{R} e^{-\mu\rho\cos\vartheta} \sin\vartheta \, d\vartheta \, dr} \tag{19}$$

R = sample radius

$\mu\rho$ = mass absorption coefficient for gamma rays in the sample

r = distance between the centre of the sample and volume element dV where gamma rays were created

ϑ = angle between direction of radius r and spectrometer axis

We have taken into account the energy dependence of the absorption coefficient for gamma rays on the sample material.

The correction for the absorption of gamma rays in paraffin was calculated for two cases. The measurements on the elements Y and Pr were performed with the paraffin cone inserted into the

bismuth collimator. The paraffin cone was replaced in the calculus by a series of concentric cylinders. In the approximation that gamma rays are directed along the axis of the spectrometer, the correction factor was obtained using equation:

$$\eta_{par} = \frac{1}{\sum_{i=1}^{n} d_i \, e^{-\mu_1 v_i}} = 1.16 \qquad (20)$$

d_i = part of gamma rays entering a particular cylinder
v_i = length of a particular cylinder
μ_1 = mass absorption coefficient for gamma rays in paraffin CH_2

$$\mu_1 = \varrho_{par} \cdot \left[\frac{6}{7} \mu_C + \frac{1}{7} \mu_H \right] = 1.15 \ \text{cm}^{-1}$$

The absorption coefficient for gamma rays in paraffin was not considered to be energy dependent.

Most recent measurements performed on the elements Sc and Ho were done with two paraffin cylinders instead of a paraffin cone. The correction factor in this case was $\eta_{par} = 1.48$. The whole correction for the absorption of gamma rays is the product of η_{sample} and η_{par}.

$$\eta_{abs}(E) = \eta_{sample}(E) \cdot \eta_{par} \qquad (21)$$

The error of this correction factor was estimated to be $\pm$ 0.5 %.

The measured pulse height distributions S(k) corrected for the mentioned effects (background correction, unfolding, correction for the absorption of gamma rays) represents the real gamma ray spectrum $S_r(E)$. This is an energy distribution of all gamma rays which were created in the sample and were directed towards the converter of the spectrometer. Being mainly concerned with prompt radiative capture gamma rays which appear at energies above 14 MeV, we put the low energy limit of the measured spectra at about 12 MeV.

5.4. Correction of the measured number of neutrons

With previous corrections we get the exact number of gamma rays created in the sample and directed towards the converter of the spectrometer. If we want to calculate a cross section for the radiative capture of 14 MeV neutrons, we also have to know the exact number of neutrons in the sample. We cannot determine this number from measurement with the neutron monitor only, but we have to take into account processes by which neutrons interact in the sample. These processes are elastic and inelastic scattering, (n,2n) reactions and others. The effect of elastic scattering is to increase the path of neutrons in the sample or, which comes to the same thing, an increase of the effective neutron flux. This effect is estimated to be less than 1 % of total number of neutrons in the sample and is therefore negligible. All other processes treated as nonelastic processes lower the number of neutrons in the sample following the $e^{-n\delta_{non}\cdot r}$ law ($n\delta_{non}$ is the macroscopic nonelastic cross section and r is the distance from the centre of the sample to the volume element dV where capture takes place).

Correction of the neutron flux due to nonelastic processes is:

$$\eta_{flux} = \frac{S_r(E_\gamma)}{S_r''(E_\gamma)} \qquad (22)$$

$S_r(E_\gamma)$ = yield of gamma rays if nonelastic processes are taken into account following the $e^{-n\delta_{non}\cdot r}$ law

$S_r''(E_\gamma)$ = yield of gamma rays if there were no attenuation of neutron flux in the sample

In the case of measurements with spherical samples, we are also faced with an increase of neutron flux in the neutron source. This is taken into account by a factor $e^{n\delta_{non}\cdot R}$.

Correction of the measured number of neutrons is in the case of a sphere :

$$\eta_{flux} = \frac{e^{n\sigma_{non} \cdot R} - 1}{n\sigma_{non} R} \qquad (23)$$

and in the case of a hemisphere :

$$\eta_{flux} = \frac{1 - e^{-n\sigma_{non} \cdot R}}{n\sigma_{non} \cdot R} \qquad (24)$$

The effective number of neutrons from the source is then

$$I_{eff} = I_o \cdot \eta_{flux} \qquad (25)$$

I_o = number of neutrons from the neutron source in 4π from the neutron monitor measurement without correction

The error in the correction factor η_{flux} is less than $\pm$ 2 %.

6. DIFFERENTIAL AND INTEGTATED CROSS SECTION FOR THE CAPTURE OF 14 MeV NEUTRONS

The differential cross section for the radiative capture of 14.1 MeV neutrons can be obtained from real gamma ray spectrum $S_r(E_\gamma)$ and the effective number of neutrons in the sample, if we consider also the geometry of the experiment and the number of the sample nuclei in a unit volume:

$$\frac{d\sigma}{dE_\gamma} = \frac{4\pi}{\Omega^*} \cdot \frac{1}{n \cdot I_{eff} \cdot R_{eff}} \cdot S_r(E_\gamma) \left[\frac{\mu b}{0.5 \text{ MeV}} \right] \qquad (26)$$

$S_r(E_\gamma)$ = real gamma ray spectrum = $\eta_{abs} \cdot S_m(E_\gamma)$
$S_m(E_\gamma)$ = distribution obtained from $S_c(k)$ by unfolding
$S_c(k)$ = corrected measured pulse height distribution
η_{abs} = correction factor for absorption of gamma rays

R_{eff} = effective sample radius (considering a hole in the sample)
$= \frac{1}{2}(R+z - R_1 \operatorname{arctg} \frac{z}{R_1})$ for sphere

$= \frac{1}{4}(R+z - R_1 \operatorname{arctg} \frac{z}{R_1})$ for hemisphere

R = sample radius
R_1 = hole radius
z = length of the hole
I_{eff} = effective number of neutrons from the neutron source
$= I_o \cdot \eta_{flux}$
I_o = number of neutrons from the neutron source in 4π from the measurement with neutron monitor
η_{flux} = neutron number correction factor
n = density of nuclei in the sample $[cm^{-3}]$
$\frac{\Omega^*}{4\pi}$ = relative solid angle of the spectrometer
$\frac{\Omega^*}{4\pi} = 3.09 \cdot 10^{-3} (1 \pm 0.03)$

The differential cross section was calculated with the following assumptions:

- all volume elements of the sample substend an equal solid angle at the converter of the spectrometer
- gamma rays from radiative capture have an isotropic angular distribution.

Our gamma ray spectra belong to gamma rays with energies above 12 MeV. Gamma rays with energies above the incident neutron energy E_n correspond to prompt radiative capture into the bound states of the final nuclei. Gamma rays with energies below E_n correspond to (n,n'γ), (n,particleγ) and to a smaller extent to (n,γ) over unbound states. Spectra above E_n are therefore the differential cross sections for the radiative capture of 14.1 MeV neutrons into the bound states of final nuclei. Our spectra are smeared over $\Delta E_n = 1.35$ MeV which is the energy spread of incident neutrons.

Integrated cross sections are obtained from differential cross sections by integration from E_n to $E_n + B_n$, where B_n is the binding energy of the neutron in the ground state of the final nuclei:

$$\sigma_{int} = \int_{E_n}^{E_n+B_n} \frac{d\sigma}{dE_\gamma} \cdot dE_\gamma = \int_{E_n}^{E_n+B_n} \sigma(E_\gamma) \cdot \Delta E_\gamma \qquad (27)$$

7. ERRORS IN DIFFERENTIAL AND INTEGRATED CROSS SECTION

The overall error includes uncertainties due to:

- statistical errors
- the background correction 7 % for spherical samples,
  1 % for hemispherical samples
- the spectrometer response function which enlarges statistical error by a factor of 1.8
- the neutron flux 6 %
- the spectrometer efficiency 11 %
- the assumption of equal solid angle for the whole sample 1 %
- the assumption of isotropic angular distribution of γ-rays 3 %
- the energy scale uncertainties 2 % at 14 MeV,
  3 % at 22 MeV
- the correction for the absorption of γ-rays 1 %
- the correction of the neutron flux 2 %

The error of integrated cross sections include all the above mentioned uncertainities. Reported differential cross section errors include only uncertainities due to statistical errors, due to the background correction and due to the spectrometer response function, which influence the shape of the spectrum.

8. RESULTS

Experimental gamma ray spectra and integrated cross sections for radiative capture of 14 MeV neutrons in Sc, Y, Pr and Ho are presented in Table 4. Gamma ray spectra are also shown in Figs. 9, 10, 11 and 12.

All important information about targets are gathered in Table 3. Obtained integrated cross sections for Sc, Y, Pr and Ho are in accordance with results measured at other elements showing the same mass dependence (Fig. 13).

Table 3: Important data for measured elements Sc, Y, Ho, Pr

Element	Isotopic abundance	Shape	Preparation	Density (g/cm^3)	Diameter (mm)	σ_{int} (μb)
$^{45}_{21}$Sc	100%	Sphere in 0,2mm Aluminium	machining-canning	3.27	49.60 ± 0.01	800 ± 110
$^{89}_{39}$Y	100%	Sphere in 0,2 mm Aluminium	machining-canning	4.55	59.60 ± 0.02	1490 ± 210
$^{141}_{59}$Pr	100%	Sphere in 0,2 mm Aluminium	machining-canning	6.74	59.60 ± 0.005	980 ± 160
$^{165}_{67}$Ho	100%	Sphere in 0,2 mm Aluminium	machining-canning	8.83	59.61 ± 0.005	940 ± 150

Table 4: Differential and integrated cross sections for Sc, Y, Ho, and Pr

γ-ray energy (MeV)	45 Sc 21		89 Y 39		141 Pr 59		165 Ho 67	
	$\frac{d\sigma}{dE}$	error	$\frac{d\sigma}{dE}$	error	$\frac{d\sigma}{dE}$	error	$\frac{d\sigma}{dE}$	error
	μb / MeV							
11.75	329	137	1234	4o5	364	82o	332	132
12.25	163	82	4o5	169	162	418	239	92
12.75	119	65	241	139	117	277	132	62
13.25	84	49	166	98	1o4	2o1	132	57
13.75	1o4	46	119	66	165	187	175	59
14.25	115	43	172	63	3o2	179	141	48
14.75	119	4o	222	54	227	121	15o	45
15.25	1o8	32	262	49	211	97	119	37
15.75	126	34	28o	43	191	78	258	52
16.25	173	41	344	41	196	66	332	59
16.75	159	36	411	41	2o2	53	265	55
17.25	136	25	439	35	176	38	131	4o
17.75	113	17	337	27	151	29	181	42
18.25	98	13	175	18	12o	25	129	33
18.75	121	15	1o8	17	86	21	92	29
19.25	94	13	95	14	5o	16	27	16
19.75	18	5	63	13	14	9	35	23
2o.25	88	12	28	8	9	8	13	12
2o.75	56	1o	15	6	12	11	2	4
21.25	16	5	4	4	8	9	4	8
21.75	4	3	2	3	3	7	4	8
22.25	o	1	2	4	o	2	1o	12
22.75	4	5	5	6	1	5	3	6
23.25	2	4	3	6	o	1	4	1o
23.75	1	3	3	7			4	9
σ_{int} (μb)	798	115	1492	21o	983	165	939	148

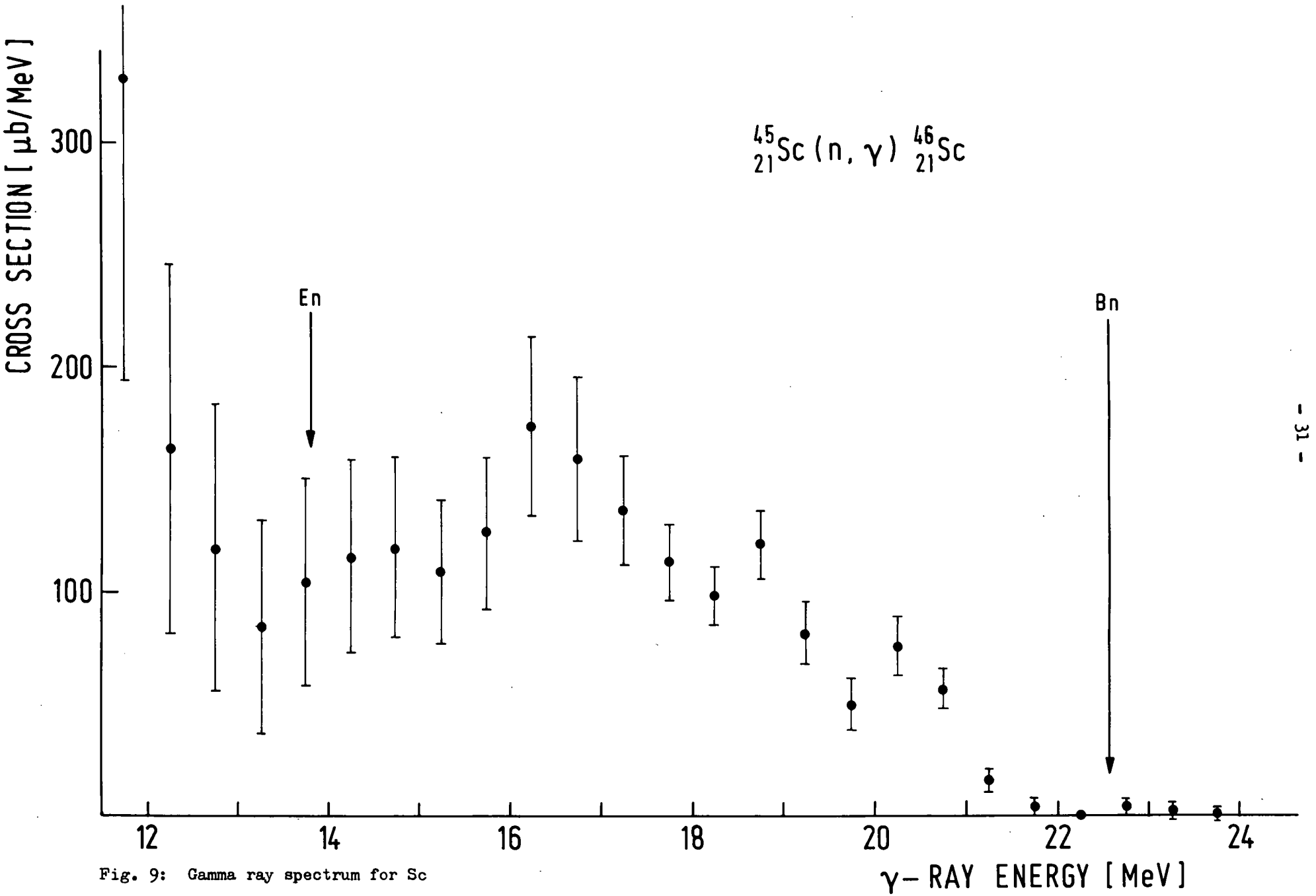

Fig. 9: Gamma ray spectrum for Sc

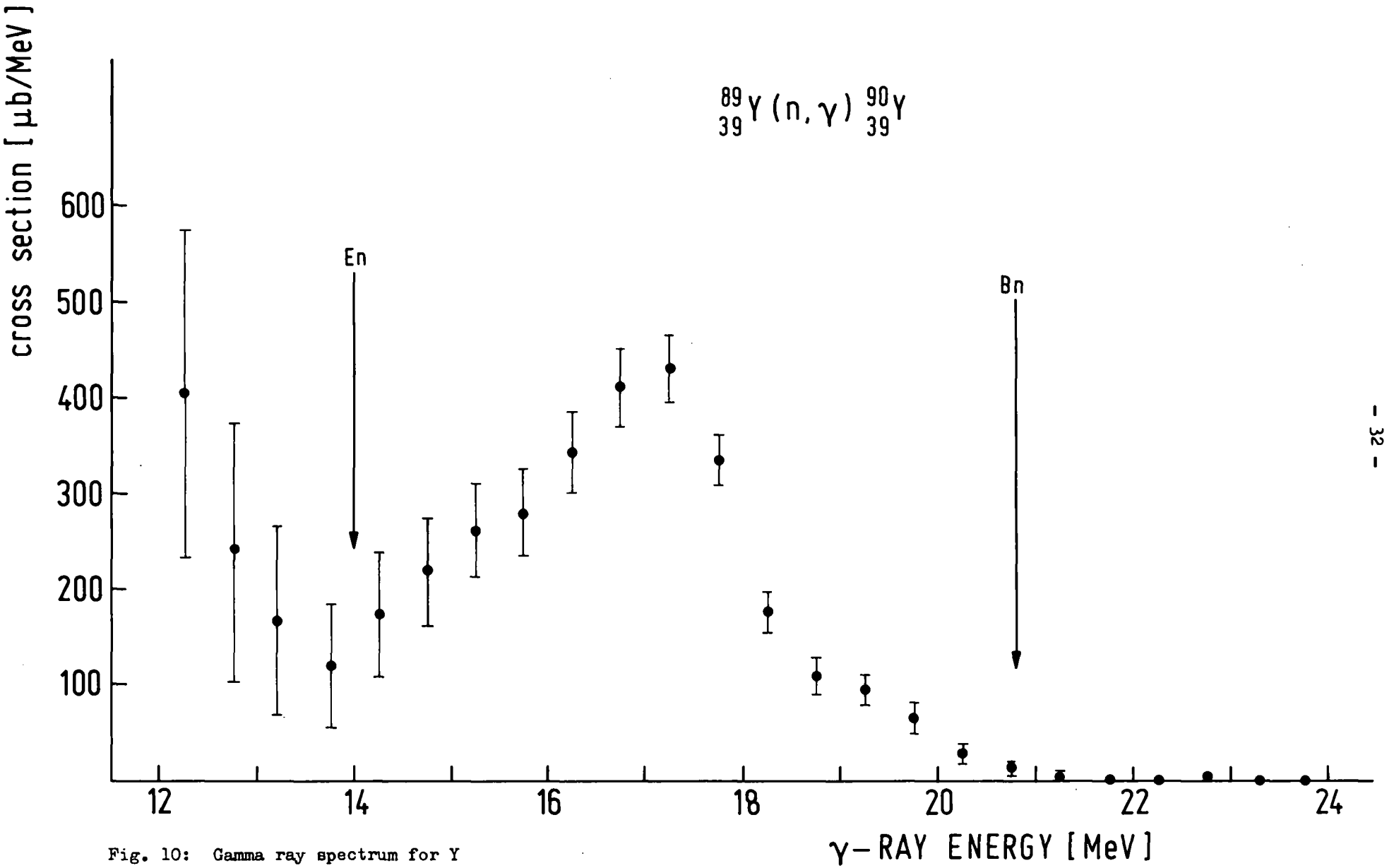

Fig. 10: Gamma ray spectrum for Y

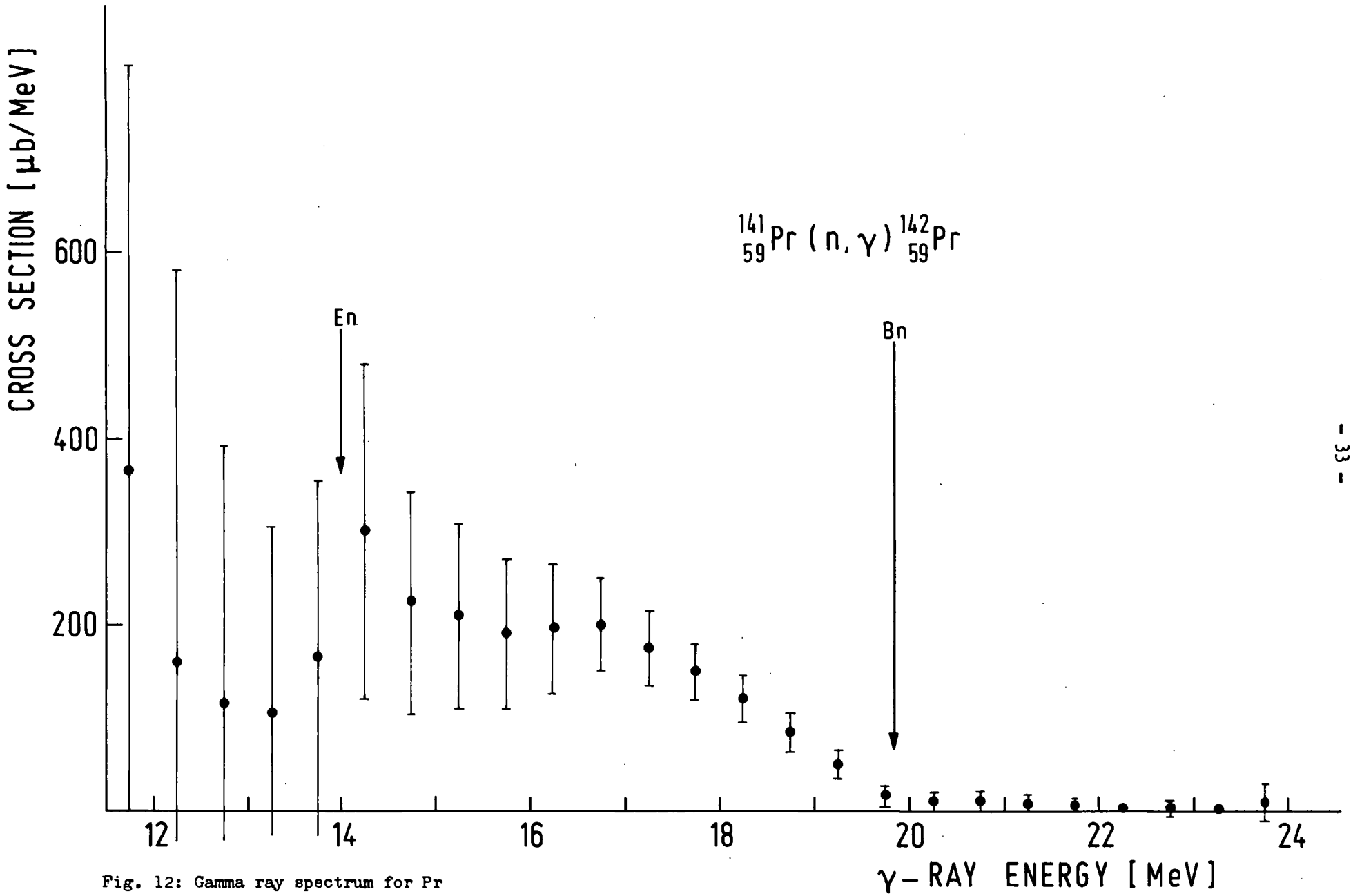

Fig. 12: Gamma ray spectrum for Pr

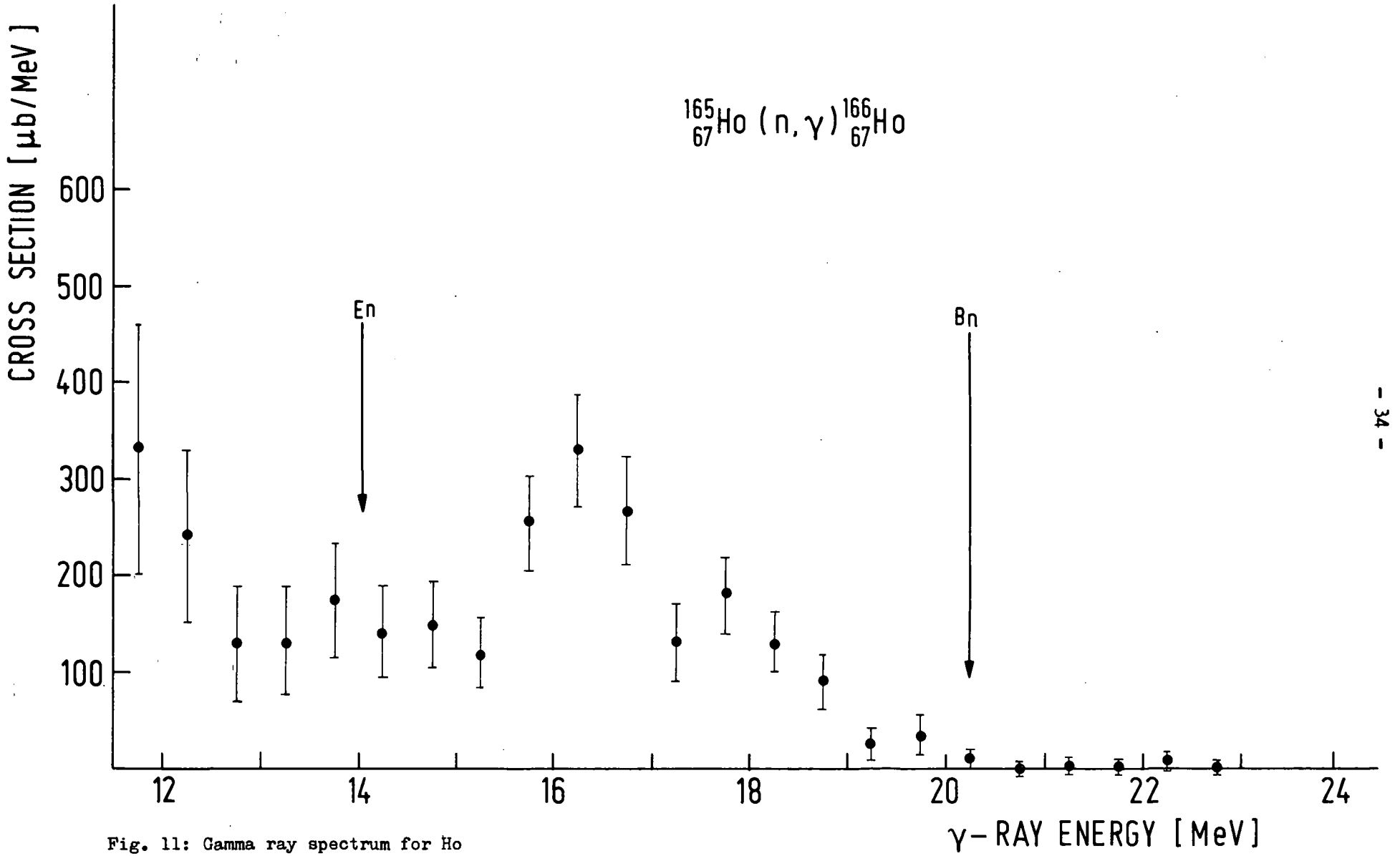

Fig. 11: Gamma ray spectrum for Ho

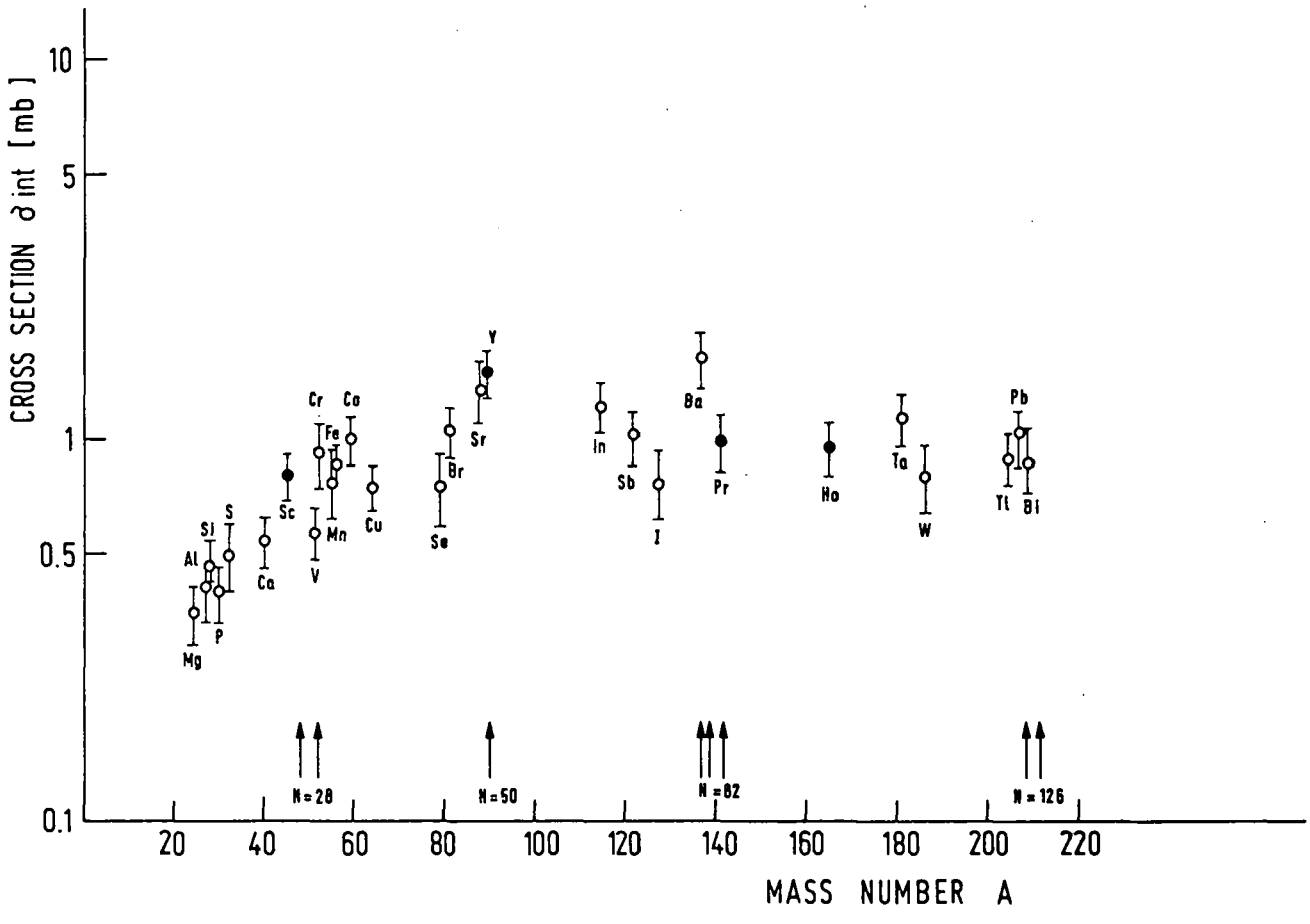

Fig. 13: Mass dependence of the integrated cross section for radiative capture of 14 MeV neutrons.

APPENDIX: EXFOR FORMAT DESCRIPTION OF THE EXPERIMENT

THIS DESCRIPTION APPEARS AS EXFOR 30364.

TITLE	GAMMA-RAY SPECTRA AND (N, GAMMA) CROSS-SECTIONS AT 14 MEV FOR SC, Y, PR, HO
AUTHOR	M.BUDNAR, F.CVELBAR, R.MARTINČIČ, A.LIKAR, M.POTOKAR
INSTITUTE	INSTITUT JOZEF STEFAN, LJUBLJANA
EXIP-YEAR	(75) MEASUREMENTS FROM 1974 TO 1976
REFERENCE	.NUCL.INSTR. METHODS OCT. 1966 (J, NIM, 44, 292, 6610) IMPROVED SPECTROMETER DESCRIBED .REPORT NIJS-R-470, NOV. 1965 (R, NIJS-R-470 , 6511) SAME AS NUCL.INS. METHODS 44(1966) 292 .NUCL.PHYS.A 130, 1969 (J, NP/A, 130, 401, 6903) DESCRIBES THE METH. NO DATA .REPORT NIJS-R-502 , JUN. 1967 (R, NIJS-R-502, 6706) DESCRIBES THE METH. NO DATA
SAMPLE	PURE ISOTOPIC COMPOSITION TARGETS ARE SPHERES (HEMISPHERES) OF 5-6 CM DIAMETER PLACED CLOSE TO THE TRITIUM TARGET. THEREFORE THE NEUTRON ENERGY IS SPREAD OVER A RANGE FROM 13.5 TO 14.7 MEV. DUE TO THIS GEOMETRY THE SPECTRA OBTAINED ARE INTEGRATED OVER A SOLID ANGLE OF 2(4) PI
STANDARD	ABSOLUTE MEASUREMENTS
FACILITY	(CCW) COCKROFT-WALTON ACCELERATOR ENERGY OF INCIDENT NEUTRONS IS=100 KEV
N-SOURCE	(D-T) T(D,N)ALPHA REACTION
INC-SPECT	THE "ENERGY-SPREAD" IS 1.35 MEV, THAT IS + - 0.675 MEV
DETECTOR	(BPAIR) SCINTILLATION PAIR SPECTROMETER WHICH RESOLUTION HAS BEEN MEASURED TO BE 12.5, 9.5 AND 8.0 PER CENT FOR GAMMAS OF ENERGIES 12.1, 16.5 AND 20.4. MEV RESPECTIVELY. EFFICIENCY , ALSO MEASURED FOR THESE GAMMA ENERGIES, HAS BEEN FOUND TO BE 0.45, 0.55 AND 0.65 PER CENT.

METHOD

GAMMA SPECTRA ARE MEASURED BY THE TELESCOPIC SCINTILLATION PAIR SPECTROMETER
RECOIL PROTON SPECTROMETER HAS BEEN USED FOR THE NEUTRON MOMITORING

CORRECTION

SPECTRA ARE CORRECTED

- FOR BACKGROUND
- FOR THE SPECTROMETER RESPONSE FUNCTION
- FOR THE GAMMAS CREATED AND ABSORBED IN THE SAMPLE
- FOR ABSORPTION OF GAMMAS IN THE PARAFFIN-COLLIMATOR
- FOR NEUTRON NONELASTIC PROCESSES IN THE TARGET

ERR-ANALYSIS

THE OVERALL ERROR INCLUDES THE UNCERTAINITY

- DUE TO STATISTICAL ERRORS
- ON THE BACKGROUND CORRECTION
  = 7 PER-CENT FOR SPHERES
  = 1 PER-CENT FOR HEMISPHERS
- DUE TO SPECTROMETER RESPONSE FUNCTION
  = ENLARGES STATISTICAL ERROR BY THE FACTOR 1.8
- ON THE ENERGY SCALE
  = 2 PER CENT AT 14 MEV
  = 3 PER CENT AT 22 MEV
- ON THE SPECTROMETER EFFICIENCY
  = 11 PER CENT
- ON THE CORRECTION FOR ABSORPTION OF GAMMAS
  = 1 PER CENT
- ON THE CORRECTION FOR NEUTRON NONELASTIC PROCESSES IN THE TARGET
  = 2 PER CENT
- ON THE NEUTRON FLUX
  = 6 PER CENT
- ON THE ANISOTROPY OF GAMMAS
  = 3 PER CENT
- DUE TO EQUAL SOLID ANGLE FOR THE WHOLE TARGET
  = 1 PER CENT

THE RESULTING ERROR FOR THE CROSS-SECTIONS IS ABOUT 15 PER CENT

ENERGY RESOL.

THE ENERGY RESOLUTION IS DETERMINED

- BY THE ENERGY WIDTH OF THE SPECTROMETER RESPONSE FUNCTION (1.65 ± 0.05) MEV
- BY THE ENERGY SPREAD OF THE NEUTRON BEAM (1.35 MEV)

THE RESULTING VALUES ARE
= 14 PER CENT AT 15 MEV
= 10 PER CENT AT 21 MEV

ANALYSIS — THE CROSS-SECTIONS ARE OBTAINED BY INTEGRATION OF THE FULLY CORRECTED GAMMA SPECTRUM OVER THE EXCITATION ENERGY INTERVAL UP TO THE BINDING ENERGY OF THE LAST NEUTRON IN THE FINAL NUCLEUS

STATUS — (APRVD)APPROVED BY BUDNAR (1/12/76)

DATA CONSTANTS

EN	EN-RSL
MEV	MEV
14.1	0.675

REFRENCES

1. A.M.Lane and J.E.Lynn, Nucl.Phys. 11 (1959) 646
2. G.E.Brown Nucl.Phys. 57 (1964) 339
3. A.A.Lushnikov, D.F.Zaretsky, Nucl.Phys.66 (1965) 35
4. C.F.Clement, A.M.Lane, J.R.Rook, Nucl.Phys.66 (1965) 273, 293
5. J.Zimany, I.Halpern, V.A.Madsen, Phys.Lett. 33B (1970) 205
6. F.Cvelbar, A.Hudoklin, Nucl.Phys. A159 (1970) 555
7. G.Longo, F.Saporetti, Phys.Lett, 42B (1972) 17
8. G.Longo, F.Saporetti, Nucl.Phys. A199 (1972) 17
9. M.Potokar, Phys.Lett.46B (1973) 346
10. M.Potokar, Thesis, University of Ljubljana, Yugoslavia (1974)
11. J.L.Perkin L.P.O'Connor and R.F.Coleman Proc.Phys.Soc. 72 (1958) 505
12. A.Poularikas, R.W.Fink, Phys.Rev. 115 (1959) 989
13. R.G.Wille, R.W.Fink, Phys.Rev. 118 (1960) 242
14. J.L.Perkin, J.Nucl.Energy 17 (1963) 349
15. E.T.Bramlitt, R.W.Fink, Phys.Rev. 13 (1963) 2649
16. J.Csikai, J.Bacsó, A.Daróczy, Nucl.Phys. 41 (1963) 316
17. P.R.Gray, A.R.Zander, T.G.Ebrey, Nucl.Phys. 75 (1966) 215
18. P.Cuzzocrea, S.Notarrigo, E.Perillo, Nuovo.Cim. 52B (1967) 476
19. H.O.Menlove, K.L.Coop, H.A.Grench, R.Sher ,Phys.Rev. 163 (1967) 1299, 1308
20. A.Paulsen, Z.Phys. 205 (1967) 226
21. H.A.Grench, K.L.Coop, H.O.Menlove, F.J.Vaughan, Nucl. Phys. A94 (1967) 157
22. J.Csikai, G.Petö, M.Buczkó, Z.Miligy, N.A.Eissa, Nucl. Phys. A95 (1967) 229
23. S.M.Quaim, M.Ejaz, J.Inorg.Nucl.Chem. 30 (1968) 2577
24. H.Dinter, Nucl.Phys. A111 (1968) 360
25. F.Cvelbar, A.Hudoklin, M.V.Mihailović, M.Najžer, V.Ramšak, Nucl.Phys. A130 (1969) 401
26. F.Cvelbar, A.Hudoklin, M.Potokar, Nucl.Phys. A138 (1969) 412

27. F.Rigand, J.Roturier, J.L.Irigaray, G.Y.Petit, G. Longo, F.Saporetti, Nucl.Phys., A154 (1970) 243

28. S.M.Quaim, J.Inorg, Nucl.Chem. 32 (1970) 1799

29. F.Cvelbar, A.Hudoklin, M.Potokar, Nucl.Phys. A158 (1970) 251

30. M.Majumder, Ind.J.Phys. 44 (1970) 204

31. F.Cvelbar, A.Hudoklin, M.V.Mihailović, M.Potokar, Fizika 2 (1970) 41

32. P.Gangrskij, I.F.Kharisov, Sov.Nucl.Phys. 12 (1971) 611

33. D.M.Drake, I.Bergquist, D.K.Mc.Daniels, Phys.Lett. 36B (1971) 557

34. F.Rigaud, J.L.Irigaray, G.Y.Petit, G.Longo,F.Saporetti, Nucl.Phys. A173 (1971) 551

35. F.Rigaud, J.L.Irigaray, G.Y.Petit, G.Longo, F.Saporetti, Nucl.Phys. A176 (1971) 545

36. E.Holub,, R.Caplar, P.Kulišić, N.Cindro, J.Vuletin, Fizika 4 (1972) 59

37. J.Kantele, M.Valkonen, Phys.Lett. 39B (1972) 625

38. M.Valkonen, J.Kantele, Nucl.Instr.Meth. 103 (1972) 549

39. I.Bergquist, D.M.Drake, D.K.Mc.Daniels, Nucl.Phys. A191 (1972) 641

40. M.Potokar, A.Likar, F.Cvelbar, M.Budnar, E.R.Hodgson, Nucl.Phys. A213 (1973) 525

41. M.Budnar, F.Cvelbar, V.Ivković, A.Perdan, M.Potokar, Fizika 5 (1973)

42. K.Ponnert, G.Magnusson, I.Bergquist, Physica Scripta 10 (1974) 15

43. F.Rigaud, M.G.Desthuilliers, G.Y.Petit, Nucl.Sci. and Eng. 55 (1974) 17

44. J.Vuletin, P.Kulišić, N.Cindro, Lettere Al Nuovo Cimento 10 (1974) 1

45. O.Schwerer, M.Winkler-Rohatsch, H:Warhanek, G.Winkler, Nucl.Phys. A 264 (1976) 105

46. F.Cvelbar, Thesis, University of Ljubljana, Yugoslavija, 1965

47. F.Cvelbar, A.Hudoklin, M.V.Mihailović, M.Najžer, Nucl. Instr. and Methods 44 (1966) 292

48. R.Martinčič, M.Sci.Thesis, University of Ljubljana, Yugoslavija, 1976

49. R.Martinčič, M.Tiringer, V.Ivković, to be published in Nucl.Instr. and Methods

50. A.Hudoklin, Thesis, University of Ljubljana, Yugoslavija, 1968

51. J.F.Mollenauer, Report UCRL-9748, 1961

Data used in the calculation of cross sections are obtained from:

1. A.H.Wapstra and N.B.Gove, Nuclear Data Tables Vol. 9 No. 4-5 (1971)

2. Handbook of Chemistry and Physics, 39th edition (1957-1958)

3. R.J.Howerton, Report UCRL-5351 (1958)

4. R.J.Howerton, Report UCRL-5226 (1958)

5. M.Abramowitz, I.A.Stegun, Handbook of Mathematical Functions, Dover Publications, Inc., New York, 1968

6. J.H.Hubbell, Report NSRDS-NBS 29 (1969)